

# Actuating Single Nano-Oscillators with Light

Sean Cormier, Tao Ding,\* Vladimir Turek, and Jeremy J. Baumberg\*

**Thermoresponsive polymers can be used to rapidly actuate individual nanoparticles forming nanomechanical oscillators. Such systems are realized here with poly(*N*-isopropylacrylamide) (PNIPAM)-coated gold nanoparticles deposited on gold films, which have a strong optical response that can be dynamically tracked. Changes in temperature surrounding the nanoparticles result in the contraction or expansion of the PNIPAM coating, thereby displacing the gold nanoparticles up and down on the gold mirror. Particle oscillation is optically monitored via the spectral position of the coupled plasmon modes, achieving sub-millisecond translocation speeds when actuated by light via plasmonic heating. These fast nano-oscillators can also generate forces exceeding 1 nN with efficiencies already exceeding 1%, which makes them ideal prototypes for nanomachines.**

For years nanoscientists have envisioned a future with nanorobots that can do surgery, scavenge cholesterol inside the body, or cooperate with existing biological nanomachines.<sup>[1]</sup> To this end, various types of nanomachines such as nanorockets,<sup>[2,3]</sup> nanoswimmers,<sup>[4,5]</sup> and nanorotors<sup>[6–10]</sup> have so far been invented, however their lack of reliable power sources, and poor controllability, slow response, and small forces have jeopardized this aim. Recently, we discovered that a hybrid system made from Au nanoparticles (NPs) and poly(*N*-isopropylacrylamide) hydrogels can exert large forces (approximately nanonewton) in a short period of time ( $\leq$ microseconds), providing an excellent candidate to drive propulsion on the nanoscale.<sup>[11]</sup> These actuating nanotransducers (ANTs) are envisioned as effective muscular sources for functional nanomachinery and are especially suitable for biological applications since they are both water soluble and biocompatible. One challenge so far however is the lack of directionality of the forces produced, making them less useful for functional mechanics.

S. Cormier, Prof. T. Ding, Dr. V. Turek, Prof. J. J. Baumberg  
NanoPhotonics Centre  
Cavendish Laboratory  
University of Cambridge  
E-mail: Cambridge CB3 0HE, UK  
E-mail: t.ding@whu.edu.cn; jjb12@cam.ac.uk

Prof. T. Ding  
Key Laboratory of Artificial Micro- and Nano-structures of Ministry of Education of China  
School of Physics and Technology  
Wuhan University  
Wuhan 430072, China

 The ORCID identification number(s) for the author(s) of this article can be found under <https://doi.org/10.1002/adom.201701281>.

DOI: 10.1002/adom.201701281

Here we explore the directionality of such forces by putting ANTs on a mirror (ANToM). The expansion and contraction of the thermoresponsive PNIPAM polymer cushions are controlled by the optically induced changes of temperature, reversibly actuating the ANT particles on the mirror up and down (Figure 1). This makes a nano-oscillator which can be used for nanomechanical devices and low-energy optoelectronic nanoswitching.

The construct is built by drop-casting PNIPAM-coated Au NPs of diameter  $2R = 80$  nm onto Au films (for details see Experimental Section). Samples are immersed in aqueous solution and covered with a glass coverslip for imaging

with dark field microscopy. The dark field spectra of individual ANToMs are collected confocally through a  $100\times$  objective (numerical aperture = 0.8) into a fiber-coupled spectrometer. Initially a heating stage placed underneath the sample controls its temperature. Heating the entire sample from 25 to 40 °C transforms the dark field image of a typical Au NP from yellow to red (lower row of Figure 1a) and the coupled plasmon peak redshifts from 590 to 645 nm (Figure 1b). The dominant color is produced by the lowest plasmonic dipole mode in the NP which interacts with its image charges in the underlying substrate, giving a coupled plasmon similar to that in a NP dimer, which is extremely sensitive to the gap size that is set by the PNIPAM coating thickness.<sup>[12–16]</sup> After the temperature cools down to 25 °C, the coupled plasmon resonance peak switches back to 590 nm again, which can be reproduced for many cycles, indicating good reversibility of this system (Figure 1c). The red-shift happens predominantly around 31 °C (Figure 1d), which agrees well with the phase transition temperature of PNIPAM (Figure S1, Supporting Information), showing the thermoresponsive actuation of PNIPAM indeed changes the gap size. The additional peak at 550 nm is from the transverse plasmon mode of the nanoparticle, and shifts much less while being obscured in the cold state. Strong hysteresis can be observed when PNIPAM is in excess (Figure S2a, Supporting Information), however this hysteresis can be minimized by removing all the free PNIPAM in solution (Figure S2b, Supporting Information).

The other reversible change that can tune the plasmon resonance is the temperature-dependent PNIPAM refractive index (from  $n_{25^\circ\text{C}} = 1.34$  to  $n_{40^\circ\text{C}} = 1.42$ ).<sup>[17]</sup> However our finite-difference time-domain (FDTD) modeling (see Experimental Section) shows this has only a minor effect on the coupled plasmons, giving red shifts of less than 15 nm (Figure 2).<sup>[18]</sup> Instead the coupled plasmon is much more sensitive to changes in gap size in cold (Figure 2a) and hot (Figure 2b) states and the

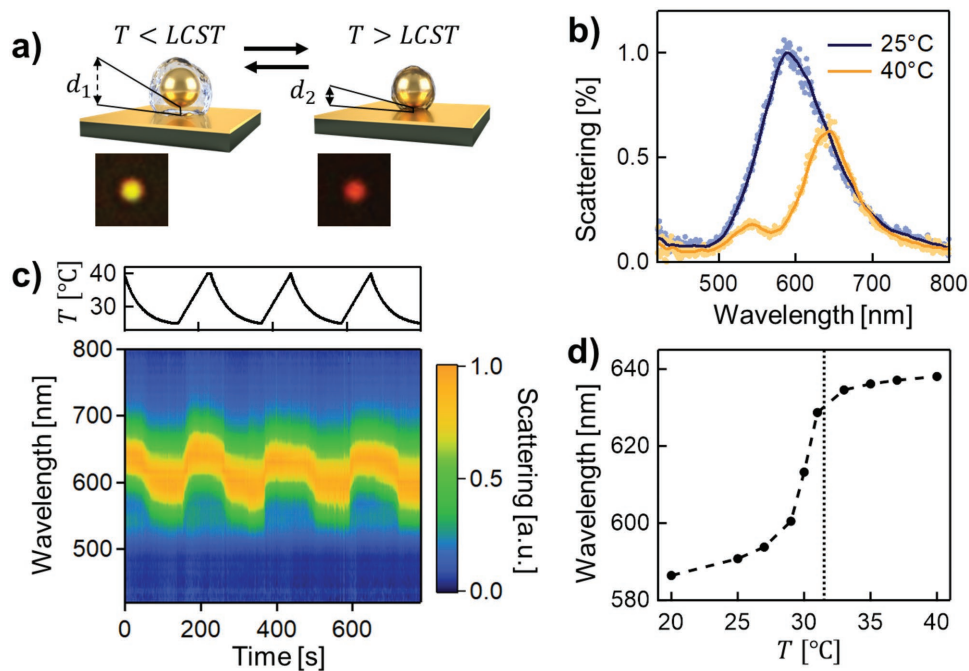


**Figure 1.** Thermal induced switching of the plasmons in ANToM. a) Schematic switching and dark field images (3  $\mu\text{m}$  square) at 25 and 40 °C. b) Scattering spectra of ANToM between 25 and 40 °C. c) Reversible switching of coupled plasmons through many cycles of heating and cooling. d) Change of the coupled plasmons while slowly ramping temperature, vertical dashed line shows measured PNIPAM phase transition temperature.

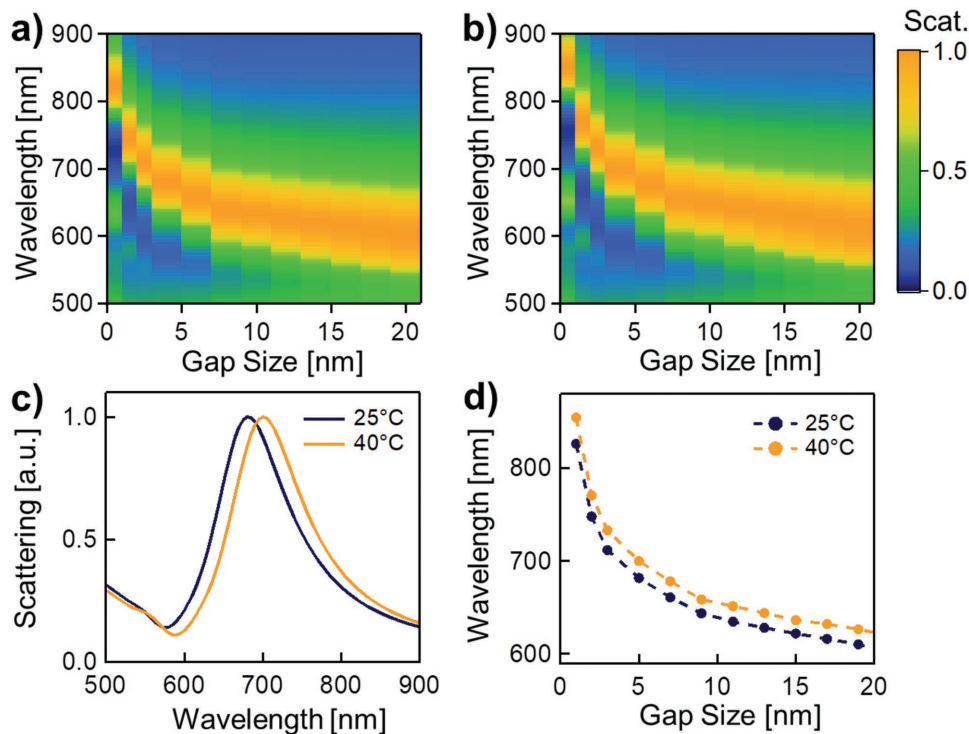


**Figure 2.** Scattering spectra from FDTD simulations of ANToM for different gap sizes at a) 25 °C ( $n = 1.34$ , cold) and b) 40 °C ( $n = 1.42$ , hot), and c) for fixed 3 nm gap with these different refractive indexes in the ANToM gap. d) Plasmon resonance wavelength versus gap size in cold (black) and hot (orange) states.

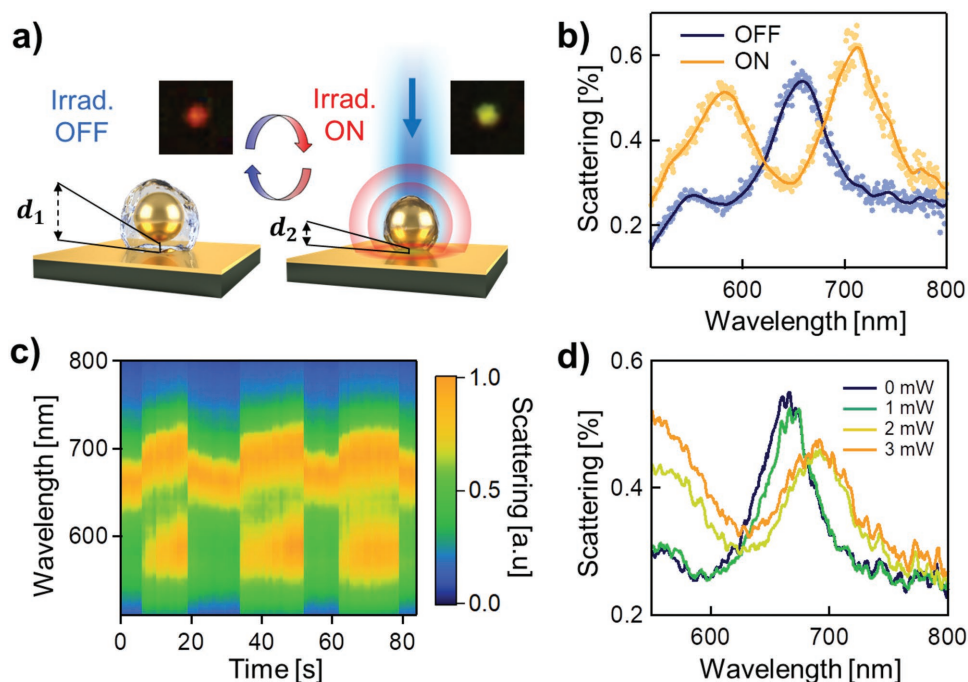


**Figure 3.** Light-induced thermal oscillation of individual ANToM. a) Schematic of switching in laser-irradiated ANToM, insets show corresponding dark-field images (3  $\mu\text{m}$  square). b) Change of scattering spectra with laser on and off. c) Switching of scattering spectra from ANToM with laser on/off over many cycles. d) Scattering spectra of ANToM at increasing irradiation powers.

observed red shift of this coupled plasmon comes mainly from the decreasing nanocavity thickness as the temperature exceeds 31  $^{\circ}\text{C}$ . Including both effects and comparing with the experimental spectra (Figure 1b), shows the gap size  $d$  decreases from  $d_1 = 20 \pm 2$  to  $d_2 = 8 \pm 1$  nm (Figure 2d). The high sensitivity of this plasmonic resonance to the nanocavity gap formed between the Au NP and Au mirror provides an ideal monitor for nano-oscillation of Au NPs.

Besides global heating of the sample, individual ANToMs can also be locally heated using a weak focused laser. Here we use a pump wavelength of 447 nm which can be easily spectrally separated, and excites the strong interband absorption of Au NPs. This efficiently transforms photon energy into thermal energy to increase the local temperature within 10 nm around the Au NP, which triggers the shrinking of PNIPAM to smaller gap size  $d_2$ . After switching off the laser, it cools rapidly and expands the gap size back to  $d_1$  (Figure 3). Cycling the laser on and off, the coupled plasmon resonance reversibly shifts between 655 and 710 nm (Figure 3b), implying repeated switching of cavity size, in this case between  $d_1 = 20 \pm 2$  and  $d_2 = 5 \pm 1$  nm. The difference in plasmon wavelengths between this NP and Figure 1b is due to its increased NP size and facets,<sup>[19]</sup> showing also the robustness of this switching to exact structure. As with the slow thermal control, this light-induced heating is highly reversible and repeatable (Figure 3c). The dynamics of switching in Figure 3c reveals both fast and slower effects. The latter possibly results from attraction of residual PNIPAM in solution onto the NP. We note the critical choice of laser power: too low a power ( $\leq 1$  mW) does not heat the gap PNIPAM above its threshold temperature, while too much power ( $> 3$  mW) can result in irreversible switching (Figure 3d).

It appears that high power lasers can damage<sup>[20]</sup> or restructure the polymer coating,<sup>[21]</sup> thereby losing its switching functionality. Optimal operation powers here of  $\approx 2$  mW  $\mu\text{m}^{-2}$  can be reduced by biasing to a higher background sample temperature just below 31  $^{\circ}\text{C}$ .

The dynamics in Figure 3c show that switching can be much faster than typical for PNIPAM systems (which mostly show transitions of seconds to minutes).<sup>[22,23]</sup> To measure the nano-oscillation rate of ANToMs we increased the modulation frequency of the continuous wave (CW) pump laser, showing their capability for sub-millisecond response (Figure 4), already more than 20 times faster than video rate. This is also very much faster than all current molecular machines.<sup>[6]</sup> Since the scattering signals from single ANToMs are small, care has to be taken to avoid any light-induced degradation in this measurement, but we find similar dynamics and spectral shifts for each of the individual ANToMs studied. As we discuss below, the fast response is mainly due to laser-induced fast heating and rapid cooling inside the sub-20 nm gap volumes, which allows water to rapidly swell the PNIPAM.<sup>[24,25]</sup>

The thermal diffusion length of water that is significantly heated around each Au NP, set by conduction, is given by

$$l_d = \sqrt{\tau \Lambda_f / C_f} \quad (1)$$

where  $C_f$  is the heat capacity (per unit volume) of water and  $\Lambda_f$  its thermal conductivity, while the characteristic cooling time of the NP is

$$\tau = \frac{R^2 C_p^2}{9 C_f \Lambda_f} \quad (2)$$

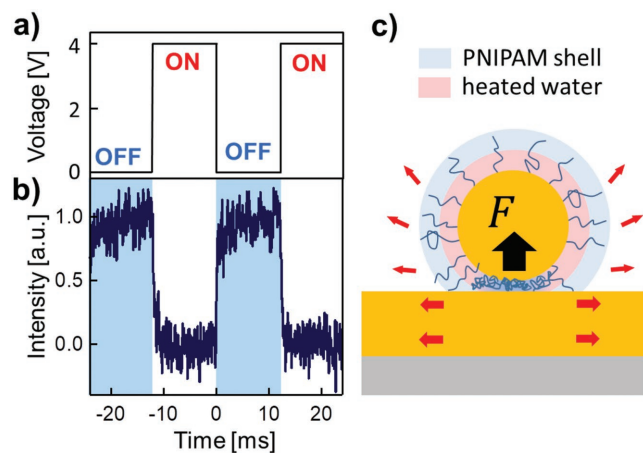


**Figure 4.** High-speed single ANToM modulation. a) Laser switching by modulating the drive voltage gives b) dynamics of dark field scattering, spectrally integrated over  $550 \text{ nm} < \lambda < 650 \text{ nm}$ . c) Expansion of collapsed PNIPAM in gap as ANToM cools below  $32 \text{ }^\circ\text{C}$ , red arrows indicate thermal conduction.

given the heat capacity of gold  $C_p$ .<sup>[26]</sup> For the nanoparticles here we thus find cooling times  $\tau \approx 440 \text{ ps}$  and thermal lengths in the water of  $l_d \approx 8 \text{ nm}$ . The geometry of the nanoparticle-on-mirror will modify these rates, since the thermal conductivity of the Au substrate is able to more efficiently wick away heat from the ANToM on top (Figure 4b). However in the cold state the NP is essentially thermally decoupled from the substrate (since  $l_d < d$ ), while in the hot state heat conduction is localized to the gap ( $l_d \approx d$ ) so that this estimate is reasonable (Figure 4b). The thermal conductivity of PNIPAM in swelled and collapsed states is not well studied, but the polymer backbone does not provide easy pathways for phonon transport and likely the main effect is to trap water which may then experience locally modified thermal conductivities. We also note that thermofluidic forces and nanoscale convection are not well studied in such nanoscale geometries, and that laminar flow will be constrained around the PNIPAM coating.

The expected timescale of the ANToM actuation may then be due to several factors besides the sub-nanosecond conduction-induced heating/cooling rates. The hydrophilic to hydrophobic phase transition that drives the swelling/collapsing of the PNIPAM in water can generate considerable forces, as discussed below. Uncoiling of the chains as they are re-solvated by water depends on diffusion through the coiled polymer layers, and is likely to occur heterogeneously. The ANToM system gives highly specific spectral information about the nanoscale geometry, as well as provide surface-enhanced Raman scattering which enhances the vibrational spectroscopy of the polymers in the gap. This is thus an ideal system in which to study in more detail the coiling and uncoiling of confined polymer chains as well as the nanoscale diffusion of water in constrained environments, making them an intriguing target for further experiments.

The forces generated from the fast expansion of the ANToM NPs on the mirror can be well estimated by considering the state just after the PNIPAM cools below its transition temperature. At this moment, the  $t = 20 \text{ nm}$  thick PNIPAM

is elastically squeezed down to  $d = 6 \text{ nm}$  with maximum strain  $e = (t-d)/t = 70\%$  which exerts a strong vertical force (Figure 4c). This resulting force can be estimated as  $F = Y_c \sqrt{R}(t-d)^{1.5}$ , where  $Y_c = 1.8 \text{ MPa}$  is the Young's modulus of PNIPAM in the cold state.<sup>[11]</sup> For the  $80 \text{ nm}$  diameter Au NP and  $20 \text{ nm}$  PNIPAM coating used here, the forces during the oscillation are  $\approx 1 \text{ nN}$ , directed away from the substrate. Unlike our previous work on ANT clusters, the calibration of these forces, which depends on extracting  $t, d$  accurately from the optical spectra, is much better defined since the individual ANToM spectra are highly sensitive to geometry and easily modelled. Forces of this order of magnitude are indeed required to overcome the Van der Waals attraction between the Au NP and the Au substrate, which is also on nanonewton levels for such small gaps and large NPs. We thus confirm the conclusion that forces exceeding  $1 \text{ nN}$  are generated, of great utility for nanoactuation.

To evaluate the energy efficiency of this nano-oscillating system defined by  $\eta = 100\% \times W/Q$ , we estimate the work done by mechanical oscillation of the Au NPs  $W \approx F(t-d) \approx 10 \text{ aJ}$  and the thermal input to heat the  $l_d = 8 \text{ nm}$  thick shell of water around the ANToM above the transition temperature by  $\Delta T = 2 \text{ }^\circ\text{C}$ , giving  $Q \approx 4\pi R^2 l_d C_p \Delta T \approx 1 \text{ fJ}$ . Therefore the efficiency of this nano-oscillator is found to be  $\eta \approx 0.1 \left(\frac{t}{R}\right)^{2.5} \approx 1\%$  which is orders of magnitude larger than any molecular machine, and approaching efficiencies for optimized macroscale machines as well as biological motors/pumps. We note that the absorption cross-section of ANToMs can be similar to the geometrical focal spot when the driving light is resonantly tuned to the plasmon and the gap size optimized,<sup>[17,27]</sup> suggesting that actuation with microwatt powers should be possible.

In summary, we demonstrate a nano-oscillating system composed of individual PNIPAM-coated Au NPs on a metal film. These are thermoresponsive and can be actuated with light, achieving switching times of order  $\mu\text{s}$ . The fast shrinking and swelling of the polymeric coating is caused by the expulsion and reabsorption of water induced by rapid, local temperature changes from plasmonic heating and passive cooling effects on the nanoscale. Monitoring the spectral shifts of the coupled plasmon resonances in this system allows the dynamics to be tracked in real time, opening up new possibilities for studying polymer chain dynamics and solvation. While such nanomechanical oscillators currently generate forces up to  $1 \text{ nN}$  with efficiencies of  $1\%$ , further optimizations are highly possible. Such light-controlled nano-oscillators open up new possibilities for building nanomechanical devices, nanogenerators, and powering of nanomachines.

## Experimental Section

**Sample Preparation:** Au NPs of average diameter  $80 \text{ nm}$  (BBI Solutions) were mixed with PNIPAM-NH<sub>2</sub> ( $5.5 \text{ kDa}$ , Sigma), and heated and cooled for a few cycles to allow them to reach an equilibrium coating. They were then drop-cast sparsely on Au or Si substrates for further optical characterization. Typically, dark field spectra were collected with a fiber-coupled spectrometer (QEPro, Ocean Optics) attached to a customized microscope (Olympus, BX51). The samples were immersed in  $50 \times 10^{-3} \text{ M}$  NaCl aqueous solution with a coverslip

on top and actuated with a heating plate underneath (Linkam) or using a focused laser (Coherent CUBE 447 nm). The laser was externally square-wave modulated and the scattering signals from individual ANTs-on-mirror were collected through a 550 nm long-pass and 650 nm short-pass edge filter before detection in a photomultiplier connected to a high speed digital storage oscilloscope (Agilent).

**Simulations:** Numerical simulations for determining the scattering cross-sections of ANToM samples were performed with Lumerical Solutions. The calculations were performed on 80 nm gold nanoparticle on top of 100 nm thick Au metal films with gap spacings from 1 to 20 nm and surrounded by a PNIPAM cladding. The dielectric functions of Au were obtained from Johnson and Christy. The calculations used a broadband plane-wave source incident normal to the gold films, in order to probe their coupled plasmonic resonances.

## Supporting Information

Supporting Information is available from the Wiley Online Library or from the author. Source data can be found at: <https://doi.org/10.17863/CAM.17410>.

## Acknowledgements

The authors acknowledge the support from EPSRC grants EP/N016920/1 and EP/L027151/1, ERC grants LINASS 320503 and ANTNAME 778616, and Leverhulme Trust (ECF2016-606). Prof. T. Ding thanks the support from the 1000-talents Youth Program and start-up grant from Wuhan University. S.C. thanks the support from the Winton Programme for the Physics of Sustainability.

## Conflict of Interest

The authors declare no conflict of interest.

## Keywords

actuators, fast switching, gold nanoparticles, nanomachines, plasmonics, PNIPAM, thermoresponsive

Received: November 27, 2017

Revised: January 8, 2018

Published online:

- [1] G. A. Ozin, I. Manners, S. Fournier-Bidoz, A. Arsenault, *Adv. Mater.* **2005**, *17*, 3011.  
 [2] Z. Wu, Y. Wu, W. He, X. Lin, J. Sun, Q. He, *Angew. Chem., Int. Ed.* **2013**, *52*, 7000.  
 [3] S. Sanchez, A. N. Ananth, V. M. Fomin, M. Viehrig, O. G. Schmidt, *J. Am. Chem. Soc.* **2011**, *133*, 14860.  
 [4] J. Katuri, X. Ma, M. M. Stanton, S. Sánchez, *Acc. Chem. Res.* **2017**, *50*, 2.  
 [5] D. Walker, M. Kübler, K. I. Morozov, P. Fischer, A. M. Leshansky, *Nano Lett.* **2015**, *15*, 4412.  
 [6] W. R. Browne, B. L. Feringa, *Nat. Nanotechnol.* **2006**, *1*, 25.  
 [7] M. Liu, T. Zentgraf, Y. Liu, G. Bartal, X. Zhang, *Nat. Nanotechnol.* **2010**, *5*, 570.  
 [8] S. K. Samanta, J. W. Bats, M. Schmittel, *Chem. Commun.* **2014**, *50*, 2364.  
 [9] L. Shao, Z.-J. Yang, D. Andrén, P. Johansson, M. Käll, *ACS Nano* **2015**, *9*, 12542.  
 [10] P. Ketterer, E. M. Willner, H. Dietz, *Sci. Adv.* **2016**, *2*.  
 [11] T. Ding, V. K. Valev, A. R. Salmon, C. J. Forman, S. K. Smoukov, O. A. Scherman, D. Frenkel, J. J. Baumberg, *Proc. Natl. Acad. Sci. USA* **2016**, *113*, 5503.  
 [12] M. Hu, A. Ghoshal, M. Marquez, P. G. Kik, *J. Phys. Chem. C* **2010**, *114*, 7509.  
 [13] C. Lumdee, S. Toroghi, P. G. Kik, *ACS Nano* **2012**, *6*, 6301.  
 [14] T. Ding, D. Sigle, L. Zhang, J. Mertens, B. de Nijs, J. J. Baumberg, *ACS Nano* **2015**, *9*, 6110.  
 [15] T. Ding, A. W. Rudrum, L. O. Turek, V. Baumberg, *Nanoscale* **2016**, *8*, 15864.  
 [16] D. O. Sigle, J. Mertens, L. O. Herrmann, R. W. Bowman, S. Ithurria, B. Dubertret, Y. Shi, H. Y. Yang, C. Tserkezis, J. Aizpurua, J. J. Baumberg, *ACS Nano* **2015**, *9*, 825.  
 [17] B. W. Garner, T. Cai, S. Ghosh, Z. Hu, A. Neogi, *Appl. Phys. Express* **2009**, *2*, 057001.  
 [18] C. Tserkezis, R. Esteban, D. O. Sigle, J. Mertens, L. O. Herrmann, J. J. Baumberg, *Phys. Rev. A* **2015**, *92*, 053811.  
 [19] F. Benz, R. Chikkaraddy, A. Salmon, H. Ohadi, B. de Nijs, J. Mertens, C. Carnegie, R. W. Bowman, J. J. Baumberg, *J. Phys. Chem. Lett.* **2016**, *7*, 2264.  
 [20] I. Aibara, S. Mukai, S. Hashimoto, *J. Phys. Chem. C* **2016**, *120*, 17745.  
 [21] T. Ding, J. Mertens, D. O. Sigle, *Adv. Mater.* **2015**, *27*, 6457.  
 [22] L.-W. Xia, R. Xie, X.-J. Ju, W. Wang, Q. Chen, L.-Y. Chu, *Nat. Commun.* **2013**, *4*, 2226.  
 [23] X. Zhang, C. L. Pint, M. H. Lee, B. E. Schubert, A. Jamshidi, K. Takei, H. Ko, A. Gillies, R. Bardhan, J. J. Urban, M. Wu, R. Fearing, A. Javey, *Nano Lett.* **2011**, *11*, 3239.  
 [24] S. Murphy, S. Jaber, C. Ritchie, M. Karg, P. Mulvaney, *Langmuir* **2016**, *32*, 12497.  
 [25] X. Chen, Y. Chen, M. Yan, M. Qiu, *ACS Nano* **2012**, *6*, 2550.  
 [26] O. M. Wilson, X. Hu, D. G. Cahill, P. V. Braun, *Phys. Rev. B* **2002**, *66*, 224301.  
 [27] R. Chikkaraddy, X. Zheng, F. Benz, L. J. Brooks, B. de Nijs, C. Carnegie, M.-E. Kleemann, J. Mertens, R. W. Bowman, G. A. E. Vandenbosch, V. V. Moshchalkov, J. J. Baumberg, *ACS Photonics* **2017**, *4*, 469.